Spectroscopy of ^{135}La

R. Leguillon,[1,2] H. Nishibata,[3] Y. Ito,[3] C. M. Petrache,[1,2] A. Odahara,[3] T. Shimoda,[3] N. Hamatani,[3] K. Tajiri,[3] J. Takatsu,[3] R. Yokoyama,[3] E. Ideguchi,[4] H. Watanabe,[5] Y. Wakabayashi,[5,6] K. Yoshinaga,[7] T. Suzuki,[8] S. Nishimura,[5] D. Beaumel,[2] G. Lehaut,[9] D. Guinet,[9] P. Desesquelles,[1] D. Curien,[10] A. Astier,[1] T. Konstantinopoulos,[1] and T. Zerrouki[1]

[1]*Centre de Spectrométrie Nucléaire et de Spectrométrie de Masse, Université Paris-Sud and CNRS/IN2P3, 91405 Orsay, France*

[2]*Institut de Physique Nucléaire, CNRS/IN2P3, 91405 Orsay, France*

[3]*Department of Physics, Osaka University, Toyonaka, Osaka 560-0043, Japan*

[4]*Center for Nuclear Study (CNS), University of Tokyo, Wako, Saitama 351-0198, Japan*

[5]*RIKEN, Wako, Saitama 351-0198, Tokyo, Japan*

[6]*Japan Atomic Energy Agency (JAEA), Tokai-mura, Ibaraki 319-1195, Japan*

[7]*Tokyo University of Science, Yamazaki, Noda, Chiba 278-8510, Japan*

[8]*Research Center for Nuclear Physics (RCNP), Osaka University, Ibaraki, Osaka 567-0047, Japan*

[9]*IPNL CNRS/IN2P3 and Université Lyon 1, 69622 Villeurbanne, France*

[10]*IPHC/DRS, Université de Strasbourg, 67037 Strasbourg, France*

(Received 13 June 2013; revised manuscript received 21 July 2013; published 8 October 2013)

The ^{135}La nucleus has been studied using the fusion-evaporation reaction ^{124}Sn(^{17}N,6n) induced by the ^{17}N radioactive beam. The level scheme has been constructed from the γ-γ coincidence measurement with an array of 12 HPGe detectors, and the lifetimes of two previously known isomeric states has been deduced. The transitions and their intensities observed in the current work as well as the level scheme derived from them is in agreement with the results of a recently published work. However, our interpretation of the results differs significantly in terms of spin and parity assignments, thus solving various contradictions concerning the configurations of some of the bands discussed in the aforementioned work.

DOI: 10.1103/PhysRevC.88.044309 PACS number(s): 21.10.Re, 21.60.Ev, 23.20.Lv, 27.60.+j

I. INTRODUCTION

The nuclei around the $N = 82$ shell closure offer a unique laboratory for the study of the shape coexistence in different spin regions, from low and medium spins where spherical and triaxial shapes compete [1,2]. These nuclei often present isomeric states which have simple multi-quasiparticle configurations and are therefore easier to interpret. However, close to the line of stability the experimental information on high-spin states is scarce, mainly due to the lack of available projectile-target combinations for the production of these nuclei through fusion-evaporation reactions. This is the case for the $A \sim 135$ nuclei with neutron numbers close to $N = 82$.

Based on the CASCADE model [3], i.e., a combined model of a one-dimensional potential model (Bass model) for fusion reactions and a statistical decay model, the highest angular momenta of the ^{135}La states populated by the fusion-evaporation reactions ^{124}Sn(^{17}N,6n) and ^{122}Sn(^{17}N,4n) are estimated to be 45$\hbar$ and 35$\hbar$, respectively, and the associated cross sections to be around 660 and 80 mb, respectively. Since the present work aims at populating high-spin states in ^{135}La, it is reasonable to use the ^{124}Sn(^{17}N,6n) reaction, instead of ^{122}Sn(^{17}N,4n). The development at Research Center for Nuclear Physics (RCNP), Osaka University, of an intense ^{17}N radioactive beam offered the possibility to populate high-spin states in nuclei close to the line of stability by inducing fusion-evaporation reactions [4].

By bombarding the heaviest stable tin isotope ^{124}Sn, we could populate high-spin states in ^{135}La via the strongly populated 6n reaction channel. The use of a radioactive beam, which is several orders of magnitude less intense than a stable beam, leads inherently for the time-being to low statistics. In order to obtain a set of data with good statistics we optimized both the radioactive ion beam production and the efficiency of the detection setup. We could therefore obtain a reasonable data set to develop the level scheme of ^{135}La and to measure the lifetime of the known isomers in this nucleus [5].

The results on ^{135}La reported in the present paper and the related interpretation are to be considered as a contribution to clarify the interpretation of the results recently reported in Ref. [6] which is in disagreement with ours.

II. EXPERIMENTAL DETAILS

High-spin states in ^{135}La have been populated through the ^{124}Sn(^{17}N, 6n) reaction with a radioactive secondary beam of ^{17}N produced using the ^{9}Be(^{18}O,^{17}N)^{10}B transfer reaction on a 40 μm thick ^{9}Be target. The ^{18}O primary beam was delivered by the AVF cyclotron of the RCNP Osaka facility at an energy of 9.2 MeV/u and an average intensity of 7 μA. The radioactive ^{17}N beam was selected using an achromatic spectrometer [7,8], achieving a maximum intensity on the target of 1.2×10^5 pps [4].

A parallel plate avalanche counter (PPAC) detecting the ions passing through was used to trigger the acquisition system. The γ rays of the residual nuclei produced by the fusion-evaporation reaction were detected with an array of 12 coaxial HPGe detectors, eight of them with anti-Compton shields, positioned at a distance of 7 cm from the target and at three different angles with respect to the beam axis: four at 50°, four at 90°, and four at 130°. The total efficiency of the array was around 3% at 1.3 MeV. A Si-ball consisting of 30 Si wafers of 170 μm thickness, with a total efficiency of around 40% for protons, was used to select the weakly populated pxn and

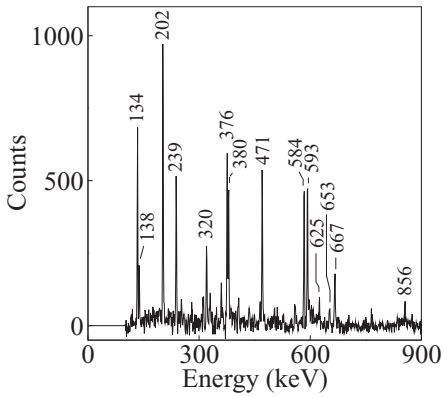

FIG. 1. Spectrum in coincidence with the PPAC and a veto on Si-ball obtained by summing the gates on the 584, 202, 593, 376, and 380 keV transitions.

αxn reaction channels (barium and cesium isotopes) from the dominating xn channels (lanthanum isotopes). The veto of the Si-ball also helped to reduce the background from the cesium and barium isotopes in the analysis of the lanthanum isotopes.

The $6n$ reaction channel leading to ^{135}La was populated with a cross section of around 0.7 b as calculated by PACE4 [9] and CASCADE [3]. The recoiling residual nuclei were stopped in the 20 μm thick ^{124}Sn target placed in the center of the γ-ray detector array to measure the prompt and isomeric decays. The repetition rate between the beam pulses of 148 ns was divided by two, leading to a beam period of 296 ns. Combined with a 0.2 ns time resolution of the CAMAC acquisition system it allowed us to extract lifetime of isomeric states by measuring the time difference between two γ-rays and/or between a γ ray and the time signal of the PPAC anode. The recorded γ-coincidence events were sorted in various two-dimensional matrices. We collected 6.5×10^7 γ events from which we could extract 2.1×10^6 γ-γ and 5.2×10^5 γ-γ-γ coincidence events. A spectrum in coincidence with the PPAC and a veto on the Si-ball, obtained by summing the gates on several transitions is shown in Fig. 1

III. RESULTS AND LEVEL SCHEME

The level scheme of ^{135}La constructed with the γ-ray transitions observed in the present experiment is shown in Fig. 3. Coincidence spectra gated on specific transitions relevant for the most intense bands are shown in Fig. 2. The experimental information on the observed transitions are given in Table I. In the present experiment we did not measure the DCO ratios and polarization asymmetries, therefore the spin-parity assignments are based on the data published in Ref. [6]. All transitions were observed previously [5,6], but important differences with respect to the recently published results in Ref. [6] are observed and presented below.

A. Spin and parity assignment to the observed states in ^{135}La

To facilitate the comparison with the level scheme of Ref. [6] we have adopted the same labeling of the bands.

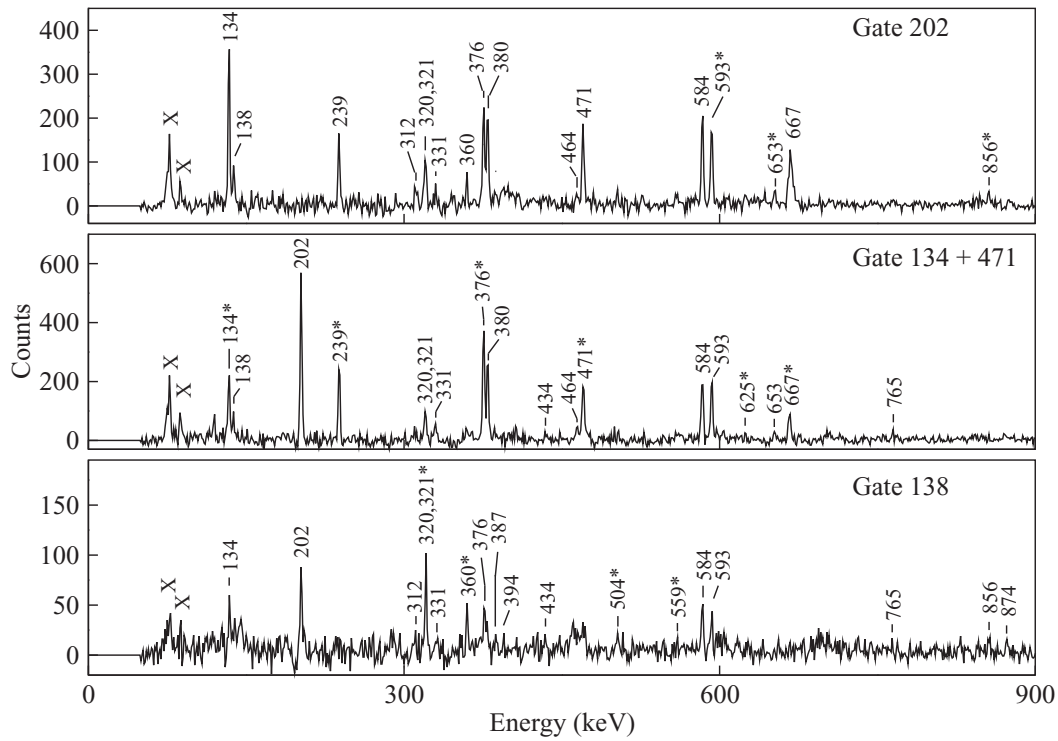

FIG. 2. Spectra in coincidence with the PPAC and a veto on Si-ball, obtained by gating on the 202 keV transition to show the transitions of band 5, on the 134 and 471 keV transitions to show the transitions of band 8, and on the 138 keV transition to show the transitions of band 6. The in-band transitions are indicated with a star symbol, while the Bi x rays from the the anti-Compton shields are indicated with an "X".

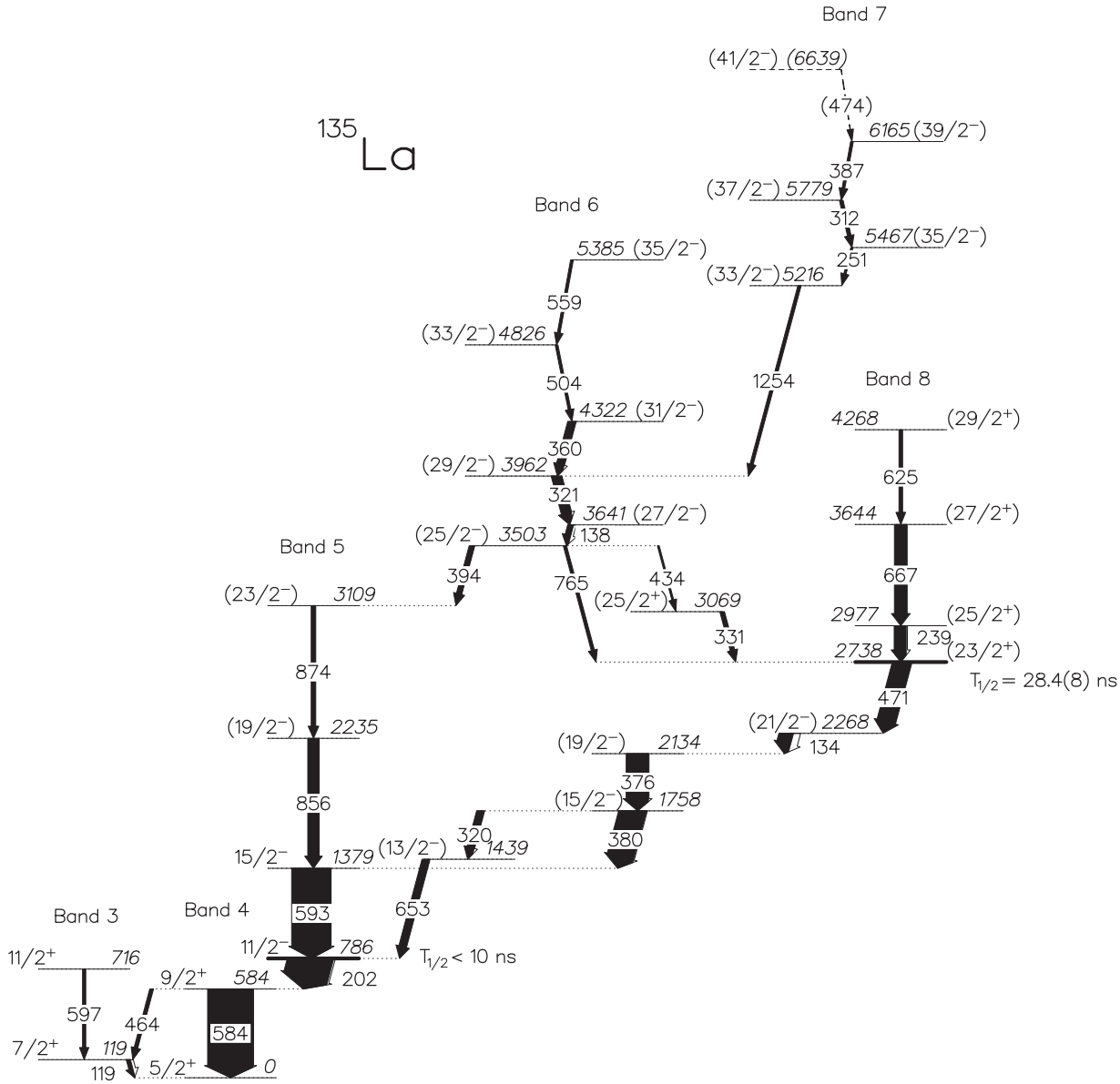

FIG. 3. Level scheme of ^{135}La resulting from the present work.

As can be seen in Fig. 3, we have drawn the transitions assigned to band 8 differently than in Ref. [6], in agreement with our interpretation of the experimental results. The first important difference with respect to Ref. [6] concerns the transitions of band 8. The band-head spin and parity of band 8 are assigned $(15/2^-)$ on the basis of the DCO ratio ($R_{\rm DCO}$) and the polarization asymmetry (Δ) of the 380 keV transition towards the yrast $15/2^-$ state, which are $1.07(3)^Q$ (the Q and D superscripts indicate the quadrupole or dipole nature of the gating transitions) and 0.19(2), respectively. The 320 keV transition from the $(15/2^-)$ band-head was too weak to allow the extraction of the $R_{\rm DCO}$ and Δ values. In the discussion of the polarization asymmetry Δ one should keep in mind that the sign of Δ for stretched and unstretched transitions is opposite [10]: for an unstretched $M1$ transition with $\Delta I = 0$ the sign is positive and for an unstretched $E1$ transition with $\Delta I = 0$ the sign is negative. The 380 keV transition has the $R_{\rm DCO}$ compatible with a $\Delta I = 2$ or $\Delta I = 0$ transition, while Δ is positive. This is in agreement with an $E2$ ($\Delta I = 2$) or $M1$ ($\Delta I = 0$) character of the 380 keV transition. In addition to the $R_{\rm DCO}$ and Δ values, the decay of the $(15/2^-)$ state at 1758 keV can help to disentangle between these two multipolarity assignments. If we assign a $\Delta I = 2$ multipolarity to the 380 keV transition, one obtains a spin-parity $19/2^-$ for the state at 1758 keV, which would decay through an unrealistic $M3$ transition of 320 keV towards the $13/2^-$ state. We therefore conclude that the 380 keV transition has $\Delta I = 0$ $M1$ character and leads to spin-parity $(15/2^-)$ for the state at 1758 keV.

The 376 keV transition of band 8 is assigned as an $\Delta I = 0$ transition in Ref. [6], leading to spin-parity $(15/2^-)$ for the state at 2134 keV. This assignment takes into account the $R_{\rm DCO} = 1.11(3)^Q$ and the positive polarization asymmetry $\Delta = 0.18(1)$ of the 376 keV transition, which are in agreement

TABLE I. Energies, intensities (corrected for detector efficiency and internal conversion), and spin-parity assignments of γ-ray transitions of ^{135}La. The transitions are grouped in bands and the transitions connecting a given band to low-lying states are listed at the end of each band separated by a blank line.

γ-ray energy(keV)	E_i(keV)	Intensity	$J_i^\pi \rightarrow J_f^\pi$
Band 3			
596.5(3)	716	7(2)	$11/2^+ \rightarrow 7/2^+$
119.2(2)	119	15(4)	$7/2^+ \rightarrow 5/2^+$
Band 4			
583.8(1)	584	100(12)	$9/2^+ \rightarrow 5/2^+$
464.3(2)	584	10(3)	$9/2^+ \rightarrow 7/2^+$
Band 5			
592.5(1)	1379	86(12)	$15/2^- \rightarrow 11/2^-$
856.0(1)	2235	25(4)	$(19/2^-) \rightarrow 15/2^-$
873.9(1)	3109	10(5)	$(23/2^-) \rightarrow (19/2^-)$
202.4(1)	786	102(16)	$11/2^- \rightarrow 9/2^+$
652.5(2)	1439	17(2)	$(13/2^-) \rightarrow 11/2^-$
Band 6			
138.3(1)	3641	18(4)	$(27/2^-) \rightarrow (25/2^-)$
320.8(1)	3962	23(7)	$(29/2^-) \rightarrow (27/2^-)$
360.3(2)	4322	18(3)	$(31/2^-) \rightarrow (29/2^-)$
503.6(3)	4826	6(2)	$(33/2^-) \rightarrow (31/2^-)$
559.0(2)	5385	6(2)	$(35/2^-) \rightarrow (33/2^-)$
394.2(2)	3503	12(4)	$(25/2^-) \rightarrow (23/2^-)$
433.8(3)	3503	4(2)	$(25/2^-) \rightarrow (25/2^+)$
764.8(2)	3503	7(4)	$(25/2^-) \rightarrow (23/2^+)$
Band 7			
251.4(4)	5467	5(1)	$(35/2^-) \rightarrow (33/2^-)$
311.5(1)	5779	8(4)	$(37/2^-) \rightarrow (35/2^-)$
386.6(3)	6165	6(3)	$(39/2^-) \rightarrow (37/2^-)$
(473.8(3))	(6639)	<2	$(41/2^-) \rightarrow (39/2^-)$
1253.9(2)	5216	7(2)	$(33/2^-) \rightarrow (29/2^-)$
Band 8			
133.9(1)	2268	46(10)	$(21/2^-) \rightarrow (19/2^-)$
238.6(2)	2977	29(7)	$(25/2^+) \rightarrow (23/2^+)$
330.7(3)	3069	10(4)	$(25/2^+) \rightarrow (23/2^+)$
375.8(1)	2134	50(10)	$(19/2^-) \rightarrow (15/2^-)$
470.6(1)	2738	42(8)	$(23/2^+) \rightarrow (21/2^-)$
666.5(1)	3644	28(5)	$(27/2^+) \rightarrow (25/2^+)$
624.7(1)	4268	8(2)	$(29/2^+) \rightarrow (27/2^+)$
319.8(1)	1758	17(9)	$(15/2^-) \rightarrow (13/2^-)$
379.5(2)	1758	61(12)	$(15/2^-) \rightarrow 15/2^-$

with either $\Delta I = 2$ $E2$ or $\Delta I = 0$ $M1$ character. It is assigned as a $\Delta I = 0$ transition in Ref. [6], ignoring the unrealistic consequences induced by this assignment. In fact, the $\Delta I = 0$ assignment for the 376 keV transition is based on two weak and questionable arguments. The first one is that the $R_{\rm DCO}$ value of the 376 keV transition is similar to that of the $\Delta I = 0$ 380 keV transition, which cannot be considered conclusive since an analog statement is also valid if the 376 keV transition has a $\Delta I = 2$ multipolarity. The second argument is the consistency with the spin-parity of the higher-lying band 6, which is also non conclusive, since the spin-parity of band 6 can be obtained consistently through a different multipolarity assignment of the other transitions assigned to band 8, as discussed in the following. Moreover, the $\Delta I = 0$ $E2$ assignment for the 376 keV transition would lead to a third $15/2^-$ state, which is expected to be weakly populated. This is in contradiction with the observed strong population of the 2134 keV state. It is therefore rather natural to assign a spin-parity $(19/2^-)$ to the 2134 keV state.

The next 134 keV transition in band 8 has $R_{\rm DCO} = 1.72(6)^D$ and is assigned as a $\Delta I = 2$ $E2$ transition, which is in disagreement with an expected $R_{\rm DCO} \sim 2.0^D$ within the quoted errors. Moreover, in Ref. [6], a 132 keV transition is reported with $R_{\rm DCO} = 1.63(6)^D$ which is similar to that of the 134 keV transition which is assigned as a $\Delta I = 1$ $M1$ transition. It is contradictory that two transitions with similar $R_{\rm DCO}$ are assigned different multipolarities. We assign therefore the 134 keV transition de-exciting the state at 2268 keV as a $\Delta I = 1$ $M1 + E2$ transition with a large mixing ratio, as indicated by the $R_{\rm DCO} = 1.72(6)^D$ value which is much higher than 1, the expected value for a pure $M1$ transition.

The 471 keV transition populating the $(21/2^-)$ state at 2268 keV has $R_{\rm DCO} = 1.04(4)^D$ and $\Delta = 0.03(1)$, which indicates an $E1$ transition leading to spin-parity $(23/2^+)$ for the initial state. This is again in contradiction with the $Q + D$ multipolarity and $23/2^{(-)} \rightarrow 19/2^{(-)}$ assignment proposed in Ref. [6]. We finally obtain the same spin value of 23/2 for the state at 2738 keV as that reported in Ref. [6], but an opposite parity, i.e., positive.

The next three transitions on top of the $(23/2^+)$ state with energies of 239, 667, and 625 keV are all $\Delta I = 1$ $M1$ transitions, leading to spin-parity $(25/2^+)$, $(27/2^+)$, and $(29/2^+)$ for the states at 2977, 3644, and 4268 keV, respectively. The $(23/2^+)$ state at 2738 keV is also populated by the 765 keV transition which has $R_{\rm DCO} = 0.50(2)^Q$ and $\Delta = 0.15(3)$, clearly indicating a $\Delta I = 1$ $E1$ transition leading to a state with spin $(25/2^-)$ at an energy of 3503 keV. The $E1$ character of the 765 keV transition is again in contradiction with the $M1$ character assigned in Ref. [6], but accidentally leads to the same spin-parity for the $25/2^-$ state at 3503 keV.

B. Lifetimes of the $11/2^-$ and $(23/2^+)$ states

Several methods based on time difference spectra were used to extract the lifetimes of the $11/2^-$ and $(23/2^+)$ states at excitation energies of 786 and 2738 keV, respectively. Before this work the lifetime of the $11/2^-$ state was known to be smaller than 20 ns [11], while the reported lifetime of the $(23/2^+)$ state was 50 ns in Refs. [12,13] and 25.9(15) ns in Ref. [5].

1. Lifetime of the $(23/2^+)$ state

The half-life of the $(23/2^+)$ isomer at 2.738 MeV was revised to be 28.4(8) ns, which is much more precise than the reported values of 50 ns [12,13] and 25.9(15) ns [5]. The improvement was due to the use of beam timing (PPAC) and taking into account the detector time resolution which is comparable with the half-life. The time spectrum between the beam and the 471 keV γ ray, which depopulates the isomer, is shown in Fig. 4. No delayed component was observed for

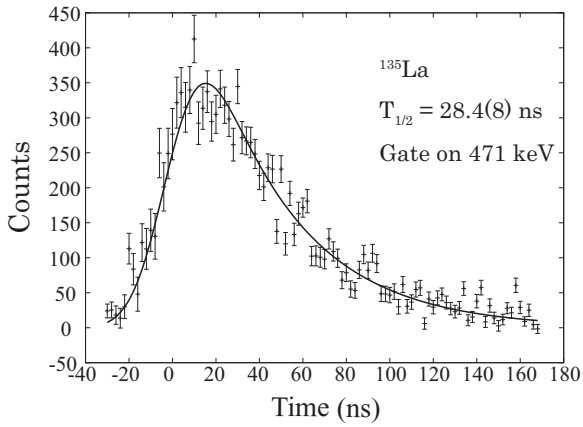

FIG. 4. Time spectrum between the beam (PPAC) and the 471-keV γ ray depopulating the isomer in ^{135}La.

the 239, 331, and 667 keV transitions feeding the $(23/2^+)$ state. The 765 keV transition was too weak to create a time spectrum and anyhow has a negligible contribution to the feeding of the $(23/2^+)$ isomer. The fitting was performed with an exponential convoluted with a gaussian function which represents the detector resolution of 32 ns (FWHM) at 471 keV. The chi-square value was examined in a two dimensional plane of the amplitude vs. the half-life, as shown in Fig. 5. The half-life of 28.4 ns was determined from a least chi-square condition and the error of 0.8 ns was estimated from an ellipse corresponding to an 1σ error limit.

2. *Lifetime of the* $11/2^-$ *state*

The population of the $11/2^-$ isomeric state by the $(23/2^+)$ isomer decay with lifetime of the same order of magnitude as that of the $11/2^-$ state prohibits the direct use of the time difference spectra between the γ rays de-exciting the $11/2^-$ state and the beam timing signal from the PPAC. To overcome this difficulty, time difference spectra were produced between all couples of Ge detectors. To increase the statistics of the

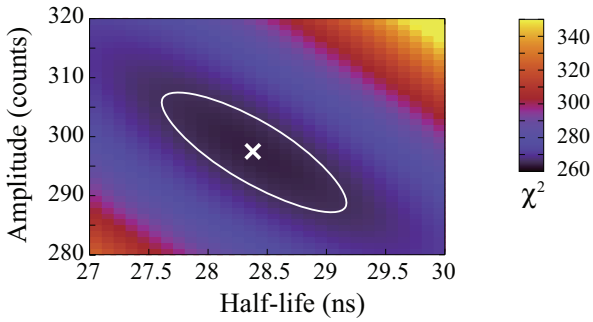

FIG. 5. (Color online) Contour plot of the chi-square value as a function of the amplitude and the half-life. The minimum chi-square value shown by a cross is obtained with a half-life of 28.4 ns. The reduced chi-square value of 2.69 demonstrates a reasonable fitting. The white circle shows an ellipse corresponding to the region where the chi-square values are 2.3 larger than the minimum one, showing an 1σ error limit.

spectra, several γ-rays above the $11/2^-$ isomer were used as start, with energies of 593, 653, 376, 380, and 471 keV, while the stop was given by the 202 keV transition de-exciting the $11/2^-$ state. For the determination of a lifetime comparable with the time resolution of the experimental setup of 32 ns (FWHM) at 471 keV, the slope method where the straight line of the decay obtained in a semilogarithmic plot is fitted, is not applicable, because there are not enough data points to fit the straight line. The centroid shift method (CSM) is independent of the time distribution slope. This statistical method is the proper technique to extract life time shorter than the time resolution [14]. When the lifetime is of the same order of magnitude or longer than the FWHM of the prompt response function, a fit of the slope can give good results, as in the case of the $(23/2^+)$ isomer discussed below. When the lifetime is shorter than the time resolution of the setup, as in the case of the $11/2^-$ state, only the CSM technique can give reasonable results. We have applied the CSM technique to the $11/2^-$ state, but for checking the reliability of the method, we also applied it to the $(23/2^+)$ state for which we obtained $T_{1/2} = 25(5)$ ns, which is in agreement with previous published results and with the more precise results obtained from $\Delta T_{\mathrm{PPAC-Ge}}$ time difference spectra (see Sec. III B 1). The experimental time

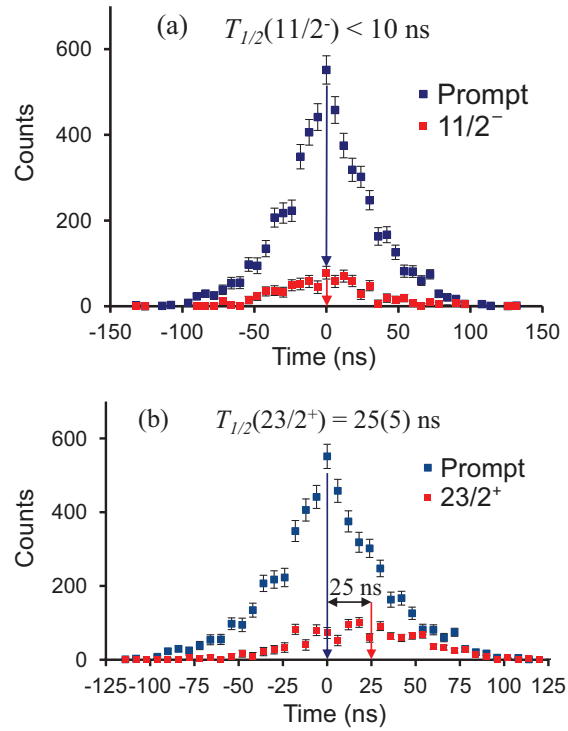

FIG. 6. (Color online) Time spectra between two γ rays populating and de-exciting the $11/2^-$ and $(23/2^+)$ states in ^{135}La. The prompt time distribution was generated summing the time difference spectra of two groups of prompt transitions: (239, 667, 625) keV and (134, 471, 376, 380) keV. The time distribution of the $11/2^-$ state was obtained as the time difference between the (134, 380, 376, 471, 593, 653, 856) keV transitions and the 202 keV transition. The time distribution of the $(23/2^+)$ state was obtained as the time difference between the (239, 667, 625) keV transitions and the (134, 471, 376, 380) keV transitions.

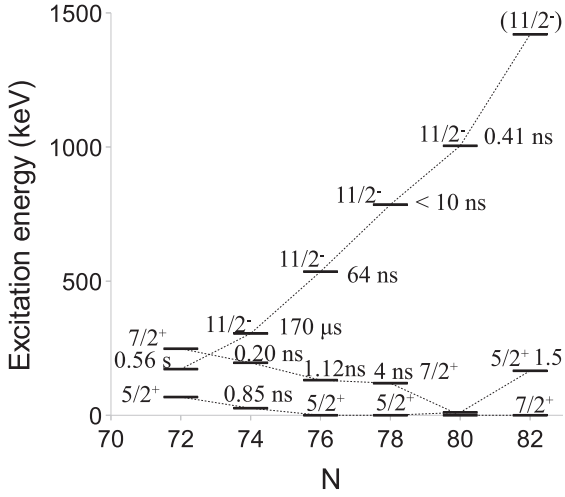

FIG. 7. Systematic of the $5/2^+$, $7/2^+$ and $11/2^-$ in the lanthanum isotopes [15–19].

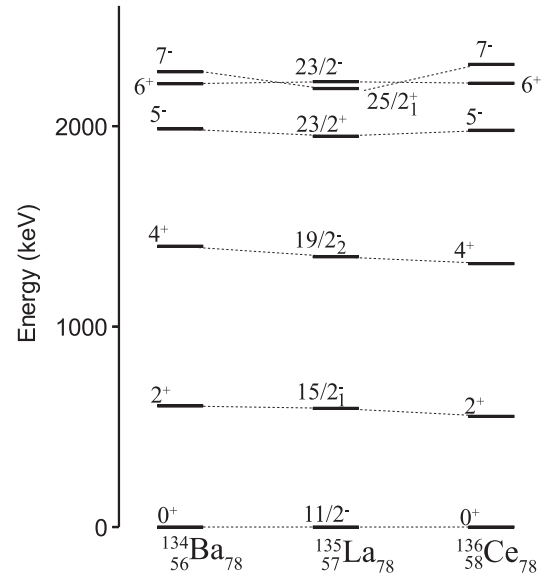

FIG. 8. Comparison between the low-lying states of ^{135}La and of the two neighboring even-even isotones ^{134}Ba [21,22] and ^{136}Ce [23].

difference spectra for the $11/2^-$ and $(23/2^+)$ states are shown in Fig. 6, in which also time difference spectra for prompt transitions are shown for comparison.

The centroid shift method allowed us to reduce the upper limit on the lifetime of the $11/2^-$ isomer to 10 ns, which fits well in the systematics of the isomeric states in the Lanthanum isotopes, as shown in Fig. 7, and gives a good guide for possible future lifetime measurements.

IV. DISCUSSION

A discussion of the observed bands of ^{135}La and a comparison with the neighboring $N = 78$ nuclei ^{137}Pr, ^{139}Pm, and ^{141}Eu can be found in Ref. [5], while an interpretation of band 6 of ^{135}La has been recently published in Ref. [6]. We will focus our attention to the interpretation of band 8, which has a different structure than that reported in the previous papers [5,6]. The previously reported band 8 cannot be considered as a band, since it consists of only one transition of 376 keV. We have three states with negative parity, the first with spins $15/2^-$ which is nonyrast, while the second and third ones with spins $(19/2^-)$ and $(21/2^-)$ are yrast. At higher spins we have three states with positive parity and spins $(23/2^+)$, $(25/2^+)$, $(27/2^+)$ which are all yrast, and finally the nonyrast $(29/2^+)$ state de-excited by the 625 keV transition.

The strongly populated $(15/2^-)$ and $(19/2^-)$ states at 1758 and 2134 keV, respectively, have been discussed in the framework of the triaxial rotor model, deducing an asymmetry parameter $\gamma \approx 25^\circ$ [13]. In the shell model approach the configurations of the yrast $15/2^-$ and $(19/2^-)$ states can be understood as the coupling of one proton in $\pi h_{11/2}$ and two protons in the $\pi(d_{5/2}g_{7/2})$ orbitals coupled to spin 2^+ or 4^+, respectively. The presence of low-lying configurations involving two protons in the $\pi(d_{5/2}g_{7/2})$ orbitals is expected, since the lowest-lying bands of ^{135}La are built on $5/2^+$ and $7/2^+$ band heads, which have configurations based on the $\pi(d_{5/2}g_{7/2})$ orbitals [6]. The strong 380 keV transition connecting the two $15/2^-$ states can be understood by the presence of two protons in the $\pi(d_{5/2}g_{7/2})$ orbitals in the configurations of both states.

The $(21/2^-)$ state can be built on a $\pi g_{7/2} \otimes \nu(h_{11/2}d_{3/2})$ maximum aligned configuration, which is expected to be yrast. Such a configuration could also induce an isomeric character for the $(21/2^-)$ state, with a lifetime similar to that of the $(23/2^+)$ state, which has not been observed experimentally due to the scarce statistics.

The isomeric $(23/2^+)$ state can be built on the $\pi h_{11/2} \otimes \nu h_{11/2}(s_{1/2}d_{3/2})^1$ configuration, which account for the $E1$ 471 keV transition which occurs between the opposite parity $\Delta l = 1$ $\pi h_{11/2}$ and $\pi g_{7/2}$ orbitals. We expect the existence of such yrast states with three quasiparticle configurations involving one proton in $\pi h_{11/2}$ with two neutrons in $\nu h_{11/2}$ and $\nu(s_{1/2}d_{3/2})^1$. States with configurations based on $\nu h^1_{11/2}(s_{1/2}d_{3/2})^1$ in even-even nuclei and $\nu h^2_{11/2}(s_{1/2}d_{3/2})^1$ in odd-even nuclei of the $A \sim 135$ mass region are commonly found yrast and often have an isomeric character [20–25]. The energies of the low-lying states of ^{135}La are compared to the low-lying levels of the neighboring even-even isotones ^{134}Ba and ^{136}Ce in Fig. 8. One can observe a nice correspondence between the 5^- and 7^- states in ^{134}Ba and ^{136}Ce nuclei with the $(23/2^+)$ state in ^{135}La, which support the $\pi h_{11/2} \otimes \nu h_{11/2}(s_{1/2}d_{3/2})^1$ configuration assignment to this state.

The higher lying $(25/2^+)$ state is strongly connected to the $(23/2^+)$ state interpreted as based on the $\pi h_{11/2} \otimes \nu h_{11/2}(s_{1/2}d_{3/2})^1$ configuration. We can naturally assign the $(25/2^+)$ state to the maximum aligned configuration $\pi h_{11/2} \otimes \nu h_{11/2}d_{3/2}$.

V. SUMMARY

High-spin states in ^{135}La have been populated using the fusion-evaporation reaction ^{124}Sn(^{17}N,6n) induced by the ^{17}N

radioactive beam. The γ-γ coincidences measured with an array of 12 HPGe detectors allowed the study of the ^{135}La level scheme and to measure the lifetime of two previously reported isomers. New parity and spins are assigned to several states. The configurations for the different bands are discussed and contradictions present in a recently published paper on ^{135}La are solved.

ACKNOWLEDGMENTS

We acknowledge the support from RCNP for both the preparation of the experiment and for the effort to create the best conditions during the measurements. This work was supported by Japan Society for the Promotion of Science (JSPS) under the FY2011 JSPS Invitation Program for Research in Japan. We thank M. G. Porquet for useful and enlightening discussions.

[1] C. M. Petrache *et al*., Phys. Rev. C **72**, 064318 (2005); **74**, 034304 (2006).
[2] C. M. Petrache, S. Frauendorf, M. Matsuzaki, R. Leguillon, T. Zerrouki, S. Lunardi, D. Bazzacco, C. A. Ur, E. Farnea, C. Rossi Alvarez, R. Venturelli, and G. de Angelis, Phys. Rev. C **86**, 044321 (2012).
[3] F. Pülhofer, Nucl. Phys. A **280**, 267 (1977).
[4] A. Odahara *et al*. (unpublished).
[5] N. Xu, Ph.D. thesis, State University of New York, New York, 1990.
[6] R. Garg, S. Kumar, M. Saxena, S. Goyal, D. Siwal, S. Verma, R. Palit, S. Saha, J. Sethi, S. K. Sharma, T. Trivedi, S. K. Jadav, R. Donthi, B. S. Naidu, and S. Mandal, Phys. Rev. C **87**, 034317 (2013).
[7] T. Shimoda, H. Miyatake, and S. Morinobu, Nucl. Instrum. Methods Phys. Res. B **70**, 320 (1992).
[8] S. Mitsuoka, T. Shimoda, H. Miyatake, Y. Mizoib, H. Kobayashi, M. Sasaki, T. Shirakura, N. Takahashi, T. Murakami, and S. Morinobu, Nucl. Instrum. Methods Phys. Res. A **372**, 489 (1996).
[9] http://lise.nscl.msu.edu/pace4.html.
[10] D. C. Stromswold, D. O. Elliott, and Y. K. Lee, Phys. Rev. C **13**, 1510 (1976).
[11] National Nuclear Data Center, Brookhaven National Laboratory, [http://www.nndc.bnl.gov/.] the ^{135}La data last updated in 2008.
[12] J. R. Leigh, K. Nakai, K. H. Maier, F. Pülhofer, F. S. Stephens, and R. M. Diamond, Nucl. Phys. A **213**, 1 (1973).
[13] J. Chiba, R. S. Hayano, M. Sekimoto, H. Nakayama, and K. Nakai, J. Phys. Soc. Jpn. **43**, 1109 (1977).
[14] J.-M. Régis, M. Rudigier, J. Jolie, A. Blazhev, C. Fransen, G. Pascovici, and N. Warr, Nucl. Instrum. Methods Phys. Res. A **684**, 36 (2012).
[15] Y. He, M. J. Godfrey, I. Jenkins, A. J. Kirwan, S. M. Mullins, P. J. Nolan, E. S. Paul, and R. Wadsworth, J. Phys. G **18**, 99 (1992).
[16] L. Hildingsson, C. W. Beausang, D. B. Fossan, R. Ma, E. S. Paul, W. F. Piel, and N. Xu, Phys. Rev. C **39**, 471 (1989).
[17] T. Morek, H. Beuscher, B. Bochev, D. R. Haenni, T. Kutsarova, R. M. Lieder, M. Müller-Veggian, and A. Neskakis, Nucl. Phys. A **391**, 269 (1982).
[18] L. Hildingson, W. Klamra, Th. Lindblad, C. G. Linden, G. Sletten, and G. Székely, Z. Phys. A **338**, 125 (1991).
[19] J. R. Van Hise, G. Chilosi, and N. J. Stone, Phys. Rev. **161**, 1254 (1967).
[20] J. J. Valiente-Dobon *et al*., Phys. Rev. C **69**, 024316 (2004).
[21] T. Morek, H. Beuscher, B. Bochev, D. R. Haenni, R. M. Lieder, T. Kutsarova, M. Müller-Veggian, and A. Neskakis, Z. Phys. A **298**, 267 (1980).
[22] E. Dragulescu, M. Ivascu, D. Popescu, G. Semenescu, I. Gurgu, L. Marinescu, and F. Baciu, Rev. Roum. Phys. **32**, 743 (1987).
[23] S. Lakshmi, H. C. Jain, P. K. Joshi, I. Mazumdar, R. Palit, A. K. Jain, and S. S. Malik, Nucl. Phys. A **761**, 1 (2005).
[24] C. M. Petrache, R. Venturelli, D. Vretenar, D. Bazzacco, G. Bonsignori, S. Brant, S. Lunardi, M. A. Rizzutto, C. Rossi Alvarez, G. de Angelis, M. De Poli, and D. R. Napoli, Nucl. Phys. A **617**, 228 (1997).
[25] S. Bhowal, G. Gangopadhyay, C. M. Petrache, I. Ragnarsson, A. K. Singh, S. Bhattacharya, H. Hübel, A. Neusser-Neffgen, A. Al-Khatib, P. Bringel, A. Bürger, N. Nenoff, G. Schönwasser, G. B. Hagemann, B. Herskind, D. R. Jensen, G. Sletten, P. Fallon, A. Görgen, P. Bednarczyk, D. Curien, A. Korichi, A. Lopez-Martens, B. V. T. Rao, T. S. Reddy, and N. Singh, Phys. Rev. C **84**, 024313 (2011).